

Embedded Model Control for UAV Quadrotor via Feedback Linearization

*Original*

Embedded Model Control for UAV Quadrotor via Feedback Linearization / Lotufo, MAURICIO ALEJANDRO; Colangelo, Luigi; PEREZ MONTENEGRO, CARLOS NORBERTO; Novara, Carlo; Canuto, Enrico. - 49:(2016), pp. 266-271. ( 20th IFAC Symposium on Automatic Control in Aerospace ACA 2016) [10.1016/j.ifacol.2016.09.046].

*Availability:*

This version is available at: 11583/2651683 since: 2016-10-04T09:45:34Z

*Publisher:*

*Published*

DOI:10.1016/j.ifacol.2016.09.046

*Terms of use:*

This article is made available under terms and conditions as specified in the corresponding bibliographic description in the repository

*Publisher copyright*

(Article begins on next page)

# Embedded Model Control for UAV Quadrotor via Feedback Linearization

M. A. Lotufo\* L. Colangelo\* C. Perez-Montenegro\*  
C. Novara\* E. Canuto\*

\* *Department of Control and Computer Engineering, Politecnico di Torino, 10129 Torino, Italy (luigi.colangelo@polito.it)*

---

**Abstract:** This study investigates the use of the feedback linearization approach as a novel way to design the internal model for Embedded Model Control (EMC). The feedback linearization allows to collect all the non-linearities at command level. EMC, by means of a disturbance dynamics model, makes possible to estimate and then reject the non-linear terms through the control law. This idea is applied to the control of an Unmanned Aerial Vehicle: the Borea project quadrotor. Embedded Model Control methodology implies the design of an internal model (Embedded Model) coded into the control unit and running in parallel with the plant. The attitude reconstruction problem is faced by means of a state observer developed on purpose and fully integrated with the model. A two-modes control strategy is proposed in order to reject systematic sensor errors, thus enhancing the attitude estimation capability. Using a high-fidelity numerical simulator, the feasibility of the proposed control strategy was demonstrated. This indicates that a feedback linearization approach allows the extension of EMC techniques to non-linear systems control. What is more, the EMC was successfully applied to the control of the Borea quadrotor.

*Keywords:* UAV, Quadrotor, Feedback Linearization, Non-linear systems

---

## 1. INTRODUCTION

Unmanned aerial vehicles (UAVs) and, more specifically, n-copters have come to prominence in the last few years. Indeed, unmanned vehicles may have several applications in modern society, spanning from complex operations, also in potentially hazardous environments for humans to more entertaining purposes. Furthermore, UAVs have drawn great attention in the control engineering research community. This is mainly due to two reasons. First of all, designing a control for this non-linear and underactuated system can represent a stimulating challenge for control researchers. Secondly, n-copters, being typically mechanically simple and fast-prototyping devices, are widely considered as a good technology for the testing of a wide range of control algorithms and designs, also employing a wide range of sensors.

The Borea<sup>1</sup> quadrotor has been developed within the Space and Precision Automatics group (S&PA), from Politecnico di Torino, in order to test planetary landing algorithms. The Borea UAV has been endowed with a complete control system in order to control its position, velocity, and attitude. The Borea quadrotor has been equipped with a wide range of sensors: three MEMS gyroscope and accelerometers, magnetometers, a barometric altimeter, a sonar and a GPS receiver. The control system has been designed within the framework of the Embedded Model Control (EMC) methodology [Canuto et al. (2014a), Canuto et al. (2014b)] using non-linear control techniques (i.e. feedback linearization). In order to

achieve this integration, the quadrotor attitude estimation problem has been addressed. This represents a paramount step towards the integration of the sensor measurements with the feedback linearised model. To enhance the attitude reconstruction, a sensors calibration procedure is proposed, introducing a multi-mode flight control strategy. A high-fidelity simulator, based on Matlab/Simulink, has been also developed in order to test the control design safely before the experimental flight tests.

This paper is organized as follows: after a general introduction, the addressed control problem is presented in section 2, together with the feedback linearised model of the quadrotor. In section 3, there is the EMC control design. Specifically, the design of the state observer is described in 3.1, while the attitude reconstruction problem is addressed in 3.2 and the calibration algorithm is presented in 3.3. In addition, the main simulated results are presented in section 4. Finally, section 5 draws some conclusions and implications of this research.

## 2. PROBLEM STATEMENT AND DYNAMIC MODEL

The model used to describe the quadrotors dynamics is non-linear and multiple-input multiple-output (MIMO). Furthermore, the quadrotor here considered has non-tiltable propellers therefore the horizontal displacement is coupled with the quadrotor attitude. Hence, in order to follow an horizontal trajectory the controller must control the attitude (under-actuated system). For this reason, the attitude reconstruction is an important point in quadrotor UAV control. Among the several attitude observers applied to the quadrotor UAV problem, Hoffmann et al. (2010)

---

<sup>1</sup> In Greek mythology, Borea was the purple-winged god of the north wind, one of the four directional Anemoi (wind-gods).

leverages a standard Kalman approach via a sensor fusion. The concept of sensor fusion is also developed by Leishman et al. (2014). Specifically in Leishman et al. (2014) the accelerometer model and its effects are studied in-depth and the aerodynamic rotor drag is leveraged to reconstruct an attitude estimate.

Given the quadrotor dynamics, there are many possible ways to control it. Three main approaches can be found in the literature: feedback linearization, sliding control, and back-stepping [Madani and Benallegue (2006)]. In Benallegue et al. (2006), Mistier et al. (2001), Voos (2009) the quadrotor model is input-output linearised with the feedback linearization method. This method requires a full state measurement to achieve the new linear model. Therefore the design of a state observer is mandatory. In literature many state observers have been applied to a quadrotor UAV. Among them, the most common is the Kalman filter and the extended Kalman filter (EKF), as described in Alexis et al. (2011) and Sebesta and Boizot (2014), whereas in Benallegue et al. (2006) a high-order sliding mode observer is implemented. Differently, in Mistier et al. (2001) the state vector is assumed to be known. Feedback linearization method, involving high order derivative terms, implies great sensibility to sensor noises and external disturbances while the sliding control approach succeeds in overcoming some of these limitations, as appears in Lee et al. (2009). On the other side, large input gains as well as chattering phenomena affect the sliding mode controller. In Benallegue et al. (2006) the feedback linearised model, although without measurement errors, is complemented by an high-order sliding mode observer aiming at ensuring a reliable estimate of the transformed states of the linearised model. In addition, the reference state trajectory is not explicitly addresses, as in Lee et al. (2009), thus implying a possibly non-smooth state trajectory with large tracking errors while reaching the target point. Finally, in Madani and Benallegue (2006) the model, split into three interconnected subsystems, is endowed with a back-stepping control, based on Lyapunov theory, able to stabilize the whole system.

The feedback linearization approach allows to collect all the non-linearities at the command level. In our approach, based on the Embedded Model Control (EMC) Canuto et al. (2014a), Canuto et al. (2014b), such result can be greatly leveraged. Indeed, EMC encompasses a disturbance dynamics model which makes possible to compensate the unknown disturbances through the control law. In addition, a wide range of sensor models are included with proper noise and error levels. Further, also the guidance algorithm (i.e. the reference generator) is built, based on the same model used for the control algorithm.

The model of the Borea quadrotor is presented briefly. Two main reference frames have been used throughout the study. First of all, an inertial reference frame whose origin matches with the take-off point. Secondly, a body frame, centred in the quadrotor CoM, whose axes are assumed to be principal of inertia. The (1) represents the attitude matrix of the body frame with respect to the inertial frame, given an 123 Euler angles rotation sequence.

$$R_b^i(\theta) = X(\phi)Y(\theta)Z(\psi) = R_b^i(\phi, \theta)Z_\psi \quad (1)$$

The states variables are inertial position ( $\mathbf{r}$ ), velocity ( $\mathbf{v}$ ), attitude angles ( $\theta$ ) and body angular rate ( $\omega$ ). These states are collected in the state vector  $\mathbf{x} = [\mathbf{r} \ \mathbf{v} \ \theta \ \omega]^T$ .

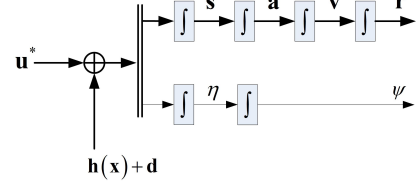


Fig. 1. Global scheme of the new equivalent model, as result of the feedback linearization.

The four available commands are the vertical acceleration in body frame ( $u_1$ ) and three angular acceleration commands ( $u_2$ ,  $u_3$ , and  $u_4$ ), about the body axes. In the feedback linearization approach, the choice of the output vector is extremely important in order to realise the input-output linearization. At this proposal, the position ( $\mathbf{r}$ ) and yaw attitude angle ( $\psi$ ) have been selected. For the sake of brevity, let us now report in (2) the result of the feedback linearization input/output procedure. The new state vector ( $\mathbf{z}$ ) is composed by the quadrotor inertial position ( $\mathbf{r}$ ), velocity ( $\mathbf{v}$ ), acceleration ( $\mathbf{a}$ ), jerk ( $\mathbf{s}$ ), yaw angle ( $\psi$ ), and its derivative ( $\dot{\eta}$ ).

$$\begin{bmatrix} \dot{\mathbf{s}} \\ \dot{\eta} \end{bmatrix} = \mathbf{B}(\mathbf{x})\bar{\mathbf{u}} + \mathbf{h}(\mathbf{x}) + \mathbf{d} \quad (2)$$

$$\bar{\mathbf{u}} = [\ddot{u}_1 \ u_2 \ u_3 \ u_4]^T, \quad \mathbf{y} = [\mathbf{r}^T \ \psi]^T$$

where  $\mathbf{B}(\mathbf{x})$  is called decoupling matrix,  $\mathbf{h}(\mathbf{x})$  collects all the non-linearities collocated at command level,  $\mathbf{d}$  represents all the possible model errors and external disturbances non-explicitly modelled. In addition, due to the needed dynamic extension, a new command vector  $\bar{\mathbf{u}}$  is introduced. Figure 1 shows the scheme of the quadrotor UAV model reported in (2) in which the command  $\mathbf{u}^* = \mathbf{B}(\mathbf{x})\bar{\mathbf{u}}$  is considered. The two integrator chains refer to the CoM position and the yaw angle dynamics.

### 3. EMBEDDED MODEL CONTROL

Starting from the **input-output** linearized model of the quadrotor in (2), a linear model-based control can be pursued. In this paper, the control of the quadrotor is performed through the Embedded Model Control (EMC) methodology. Indeed, EMC allows to treat all the non-linear effects collected in  $\mathbf{h}(\mathbf{x})$  as disturbances which can be estimated by the internal model. Moreover, these disturbances are easily cancelled by the control law since they are collocated at the command level. The EMC is based on the definition of a proper embedded model (EM) of the quadrotor. Actually, the EM is composed by a controllable dynamics plus a disturbance dynamics. The controllable dynamics is a simplified representation of the input-output dynamics. By contrast, the disturbance dynamics, being purely stochastic and parameter-free, aims at modelling the unknown disturbances and parametric uncertainties. The disturbance dynamics is driven by a noise vector playing the role of a disturbance input, to be real-time retrieved from the model error (plant output less model output) by means of a suitable noise estimator (NE). The union of the EM and the NE represents a state observer, affected by prediction errors. As a property of the EM, all the state variables, forced either by command, or noise, must be observable from the model output. By tuning the

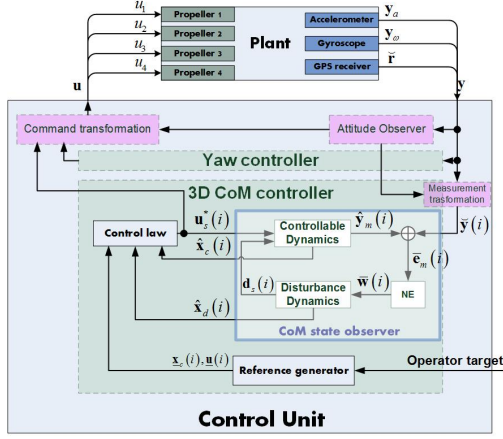


Fig. 2. EMC conceptual block diagram.

eigenvalues of the closed-loop system dynamics, the stability of the state predictor versus the neglected dynamics is achieved.

In addition, starting from the operator target, a reference generator provides the reference trajectories for command ( $\mathbf{u}$ ) and controllable states ( $\mathbf{x}_c$ ).

Finally, the control law is composed by three terms: the nominal command ( $\mathbf{u}$ ), the feedback ( $K\mathbf{e}$ ) and the disturbance rejection ( $M\mathbf{x}_d$ ):

$$\begin{aligned} \mathbf{e} &= \mathbf{x} - \mathbf{x}_c - Q\mathbf{x}_c \\ \mathbf{u} &= \mathbf{u} + K\mathbf{e} - M\mathbf{x}_d \end{aligned} \quad (3)$$

where  $\mathbf{e}$  is the tracking error, while  $Q$  and  $M$  are matrices that allow the rejection of the disturbances. The Fig. 2 sketches the overall block diagram of the EMC control unit. The command transformation block recovers the command to be dispatched to the plant  $\mathbf{u}$ , starting from the transformed command  $\mathbf{u}^*$  of the model.

### 3.1 The Embedded Model Design

The first step of the control unit design consists in building the discrete time (DT) EM, starting from the linear model in (2). In order to implement the embedded model into the DT control unit, a one-step forward Euler discretization algorithm is applied to (2). For the sake of brevity, the yaw motion dynamics has been assumed to be independently controlled. Hence, only the CoM dynamics is taken into account and addressed in this paper. As a further remark, in the case study treated here, three kinds of measurements were considered available for the control purposes: angular rates  $\mathbf{y}_\omega$  and CoM acceleration  $\mathbf{y}_a$  in body frame, and inertial position  $\hat{\mathbf{r}}$ . The CoM dynamics is complemented with appropriate disturbance state equations driven by noise vectors and estimating the noise from the model error (plant measurements minus model output). It is then viable to eliminate them from position tracking errors through disturbance rejection, under appropriate convergence conditions and sensor layout.

Figure 3 shows the block diagram of the 3D CoM state observer. As a design choice, the disturbance model of the CoM dynamics was implemented as three separated observer loops: (i) the jerk loop, (ii) the acceleration loop, and (iii) the position loop (see Fig. 3). As a matter of fact, such a model structure allowed the design to be

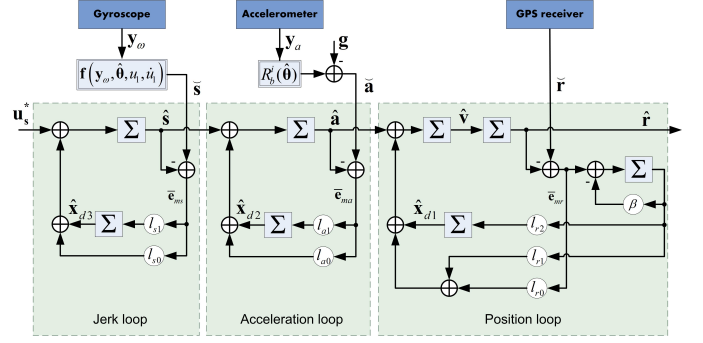


Fig. 3. 3D CoM observer.

simple but effective in leveraging the several available measurements. Indeed, given several sensors in cascade, each measure allows the estimation of the preceding loop to be corrected. For instance, accelerometer drift errors, can be corrected provided that velocity or position measurements are available. The same result cannot be achieved under pure feedback control (without disturbance rejection). In this paper, instead, the disturbance complement is designed to be fully observable. By reporting the output disturbance up to the command location it amounts to replacing systematic errors with their derivatives, as in feedback linearization. Nevertheless, some limitations may occur since derivation can force some error components, such as bias, to zero. Indeed, the latter need not to be back-stepped, but requires supplementary sensors to become real-time retrievable.

In addition, the three disturbance dynamics ( $\hat{\mathbf{x}}_{d1}$ ,  $\hat{\mathbf{x}}_{d2}$ , and  $\hat{\mathbf{x}}_{d3}$ , in Fig. 3) are able to estimate several disturbance sources. For instance, the position loop is capable of estimating the acceleration disturbances affecting the quadrotor dynamics during the flight. Such a disturbance signal is crucial to the control design being the more consistent with the physics of the phenomena under study. The correction scheme is usually implemented as a Gauss-Markov estimator, as in Kalman filtering. Error statistics must be propagated to the purpose. Systematic errors have been modelled as a first order random drift adding to the measured variable in the form of an output disturbance. A key problem is the observability of the output disturbance, which is guaranteed by supplementary and appropriate sensors.

As a further consideration, the available sensors are represented with blue blocks in Fig. 3. Since measurements are defined in their proper sensor body frames, the accelerometer and gyroscope measures were preliminary converted into the inertial frame. Such conversion requires the quadrotor attitude angles. The attitude angles were computed through a dedicated attitude state observer.

### 3.2 The Attitude Reconstruction

Given the accelerometer model in Leishman et al. (2014), the acceleration measurement (in sensor body axes) can be decomposed into:

$$\mathbf{y}_a = R_i^b(\phi, \theta, \psi)(\mathbf{a} + \mathbf{g}) + \mathbf{b} + \mathbf{e}_m \quad (4)$$

where  $\mathbf{y}_a$  is the measured acceleration in sensor body axes,  $\mathbf{a}$  is the true acceleration value,  $\mathbf{b}$  is the sensor bias and  $\mathbf{e}_m$  is the model error, including neglected dynamics and other sensor errors (mainly noises and high-frequency errors).

As a remark, in (4) the term  $\mathbf{g}$ , converted in sensor body frame, is needed because the accelerometer is not able to measure the gravity vector (see Leishman et al. (2014)). In order to use the accelerometer measurement in the input-output model in (2) (inertial frame), the formulation in (4) must be transformed in

$$\check{\mathbf{a}} = R_b^i(\hat{\phi}, \hat{\theta}, \hat{\psi})\mathbf{y}_a - \mathbf{g} \quad (5)$$

where  $\hat{\phi}$ ,  $\hat{\theta}$ , and  $\hat{\psi}$  are the estimates of the quadrotor attitude angles. Also the inertial jerk retrieval, coming from a non-linear transformation of the gyroscope measure, requires a reliable estimate of the quadrotor attitude. Hence, getting a reliable attitude estimation is one of the main problems of this study.

In order to compute the quadrotor attitude angles the acceleration estimate  $\hat{\mathbf{a}}$ , coming from the CoM state observer is considered. As a consequence, the precision of the inertial position measurement is crucial for an accurate estimation of the inertial acceleration. As a matter of fact, the error envelope of the inertial position sensor determines also the accuracy of the attitude estimation. In order to compute the attitude angles, the relation between the estimated acceleration  $\hat{\mathbf{a}}$  and the accelerometer measurement (4) is considered. By neglecting the accelerometer errors (i.e. bias  $\mathbf{b}$  and the model errors  $\mathbf{e}_m$ ), (4) reads

$$\mathbf{y}_a = R_i^b(\hat{\phi}, \hat{\theta}, \hat{\psi})(\hat{\mathbf{a}} + \mathbf{g}). \quad (6)$$

According to the attitude kinematics, (6) can be rewritten as

$$Z(\hat{\psi})\mathbf{y}_a = Y(-\hat{\theta})X(-\hat{\phi})(\hat{\mathbf{a}} + \mathbf{g}). \quad (7)$$

By assuming small attitude angles and a known yaw angle, the tilt ( $\check{\boldsymbol{\theta}} = \{\check{\phi}, \check{\theta}\}$ ) was computed after having linearized Eq. (7). The tilt angles read:

$$\check{\phi} = \frac{P_x - W_x}{W_z}, \quad \check{\theta} = \frac{P_y - W_y}{W_z} \quad (8)$$

where  $P_x$  and  $P_y$  are the first and second component of the vector  $Z(\hat{\psi})\mathbf{y}_a$ , while  $W_x$ ,  $W_y$ , and  $W_z$  are the components of the vector  $(\hat{\mathbf{a}} + \mathbf{g})$ . Nevertheless, this computed  $\check{\boldsymbol{\theta}}$  cannot be directly used to close the accelerometer loop (see Fig. 3), due to the accelerometer errors, neglected in (7). Indeed, this error terms, envisaging all the wide range of errors affecting the accelerometer measurement, would lead to a very inaccurate attitude estimate and eventually instability.

Therefore, a state observer was build in order to provide a viable estimate of the attitude tilt angles. This attitude state observer will be driven by the gyroscope measurements as input command, which are integrated in order to retrieve a rough estimate of the tilt. Further, the proposed solution, uses the attitude measure  $\check{\boldsymbol{\theta}}$  computed from a calibrated accelerometer, to counteract the attitude drift due to the gyroscope. Figure 4 shows the structure of the attitude state observer (attitude loop), according to the EMC methodology. For the sake of brevity, only the final DT equations of the attitude state observer are provided in (9).

$$\begin{aligned} \begin{bmatrix} \hat{\boldsymbol{\theta}} \\ \hat{\boldsymbol{\omega}}_d \end{bmatrix} (i+1) &= \begin{bmatrix} 1 & 1 \\ 0 & 1 \end{bmatrix} \begin{bmatrix} \hat{\boldsymbol{\theta}} \\ \hat{\boldsymbol{\omega}}_d \end{bmatrix} (i) + \bar{\mathbf{w}}(i) + T_c \begin{bmatrix} 0 \\ 1 \end{bmatrix} y_{\omega}(i) \\ \check{\boldsymbol{\theta}}(i) &= [1 \ 0] \begin{bmatrix} \hat{\boldsymbol{\theta}} \\ \hat{\boldsymbol{\omega}}_d \end{bmatrix} (i) + \bar{\mathbf{e}}_{m\theta}(i), \quad \bar{\mathbf{w}}(i) = \begin{bmatrix} l_0 \\ l_1 \end{bmatrix} \bar{\mathbf{e}}_{m\theta}(i) \end{aligned} \quad (9)$$

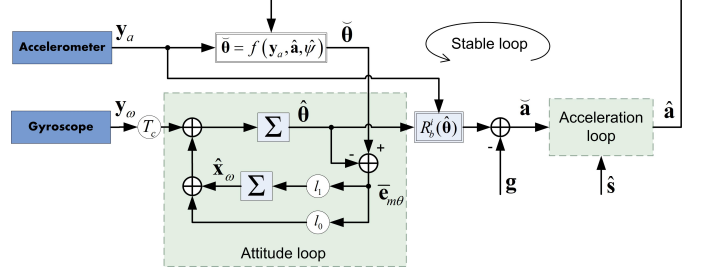


Fig. 4. Attitude feedback through attitude state observer

where  $\hat{\boldsymbol{\omega}}_d$  is the disturbance state driven by the zero-mean unpredictable noise  $\mathbf{w}$  and  $T_c$  is the time constant of the control unit. As in typical observers, the loop is closed through a static noise estimator, see  $\bar{\mathbf{w}}$  in (9). The noise estimator gains,  $l_0$  and  $l_1$  in (9) and Fig. 4, have been tuned by fixing the complementary eigenvalues of the closed-loop in order to reach a good trade-off between the loop stability and the attitude estimation performance. As mentioned above, the attitude measurement  $\check{\boldsymbol{\theta}}$  is affected by systematic errors of the accelerometer (e.g. the bias). Accelerometer bias, though very small, is such to make the attitude drifting out in a few tens of seconds, thus undermining the UAV capability in accomplishing the mission. Unfortunately, constant errors (bias) become zero through back-stepping at command level, as above mentioned. Therefore, given the designed state observers structure in Fig. 3 and Fig. 4, bias can be eliminated: (i) by disposing of supplementary sensors, (ii) by adopting calibrated sensor measurements. Hence, in order to have a reliable attitude estimate ( $\hat{\boldsymbol{\theta}}$ ) from (9), the accelerometer must be properly calibrated before closing the attitude estimation loop.

### 3.3 The Sensors calibration

A classical procedure to overcome the sensor systematic errors consists in an off-line sensor calibration. Our solution allows to avoid this additional step before starting the automatic mission phase. The proposed solution, consistently with the space missions control, consists in setting up two flight control modes: (i) calibration mode, (ii) mission mode.

In turn, the calibration envisages a double calibration process, involving both the gyroscope and the accelerometer. The gyroscope preliminary on-ground calibration aims at cancelling the gyroscope bias. The choice of an on-ground calibration is due to the easiness of the gyroscope bias identification when the quadrotor is in a no-motion condition. In addition, after the take-off, an hovering flight phase allows the accelerometer calibration. Such automatic calibration is performed by opening the attitude loop (Fig. 4) and the accelerometer loop (Fig. 3). Hence, this control mode uses only the attitude estimate obtained by the gyroscope integration.

Starting from the accelerometer model (see (4)), a reliable estimate of the accelerometer bias  $\hat{\mathbf{b}}$  can be retrieved when the quadrotor, in calibration mode, approaches a nearly-perfect hovering condition (i.e.  $\mathbf{a} = 0$  and  $R_i^b(\phi, \theta, \psi) = I$  in (4)). In this condition, an accelerometer bias estimate is

$$\hat{\mathbf{b}} = \mathbf{y}_a - \mathbf{g} \quad (10)$$

With this procedure the reliability of the bias estimation is as greater as much the hovering condition is verified. Indeed, the attitude controller must satisfy this condition as much as possible. Hovering detection can be achieved by means of applying suitable thresholds on the acceleration magnitude. Finally, the mission mode represents the operational phase of the flight. In mission mode, the attitude estimator is properly working due to the previous accelerometer and gyroscope bias calibration. Finally, as a matter of fact, also the sensors systematic errors have a time-variant behavior. This means that the initial sensor bias calibration can be considered reliable up to a certain extent. Indeed, the proposed solution can be considered viable due to the short mission time characterizing the rotating wing UAVs (in the order of 20 – 30 min) and the typical off-the-shelf sensor performance level. In any case, such limitation can be overcome through an on-line calibration which will be addressed in future studies.

#### 4. PRELIMINARY SIMULATED RESULTS

In this section some results are presented. These results have been obtained by means of a high-fidelity mission Simulink simulator. This simulator includes the dynamics of the Borea quadrotor and the models of the three sensors available on-board, affected by noise. Specifically, it is possible to simulate the dynamics of accelerometers, gyroscopes, and a differential GPS receiver. Command quantization of 12 bits was considered in the simulations. In order to test the calibration algorithm and the multi-mode control strategy (see Subsec. 3.3), a bias has been included in the simulator accelerometer measurements. It was assumed that the Borea quadrotor has a mass of 2 kg with inertia matrix  $J = \text{diag}\{0.032, 0.032, 0.061\} [\text{kgm}^2]$ , arm length equal to  $d = 0.025 \text{ m}$  and gravity constant  $g = 9.8 \text{ m/s}^2$ . Further, it has been introduced in the simulator a nearly-constant horizontal wind. The selected speed wind is about 3.5 m/s along the inertial Y-axis. From the simulation perspective, the application of the aerodynamics disturbances (force and torque) comes after the ideal partition of the quadrotor in 6 orthogonal surfaces. Such an approximation allows a quick evaluation of the main aerodynamics effects, affecting the quadrotor.

Table 1 lists the values of the complementary eigenvalues ( $\gamma_k = 1 - \lambda_k$ ) used for the 3D CoM state observer, the attitude state observer and the 3D control law. The adopted model is the same for all the three inertial axes and the same eigenvalues hold for all the three axes channels. This preliminary eigenvalues tuning allowed to reach a satisfying performance level, given the trade-off between the selected sensor errors and the desired quadrotor flight trajectory. Specifically, the eigenvalues of the attitude loop were tuned consistently with the acceleration and the position loops. Indeed, the accelerometer loop prediction error spills into the attitude observer, through the inertial acceleration estimate and the accelerometer measurement affecting  $\hat{\theta}$ . Therefore, the acceleration eigenvalues were selected in order to allow a wider bandwidth of the acceleration observer. This implies a fast and accurate enough acceleration disturbance prediction. By contrast, attitude observer bandwidth  $f_q$  must be narrower than  $f_a$ , in order to filter the measurement noise down to the gyroscope level. In turn, the position loop eigenvalues are low-frequency enough to ensure the position loop stability

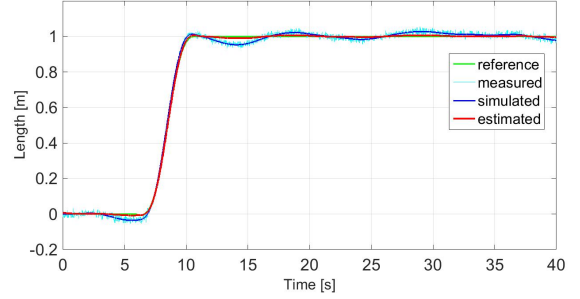


Fig. 5. Quadrotor displacement along the Y inertial axis.

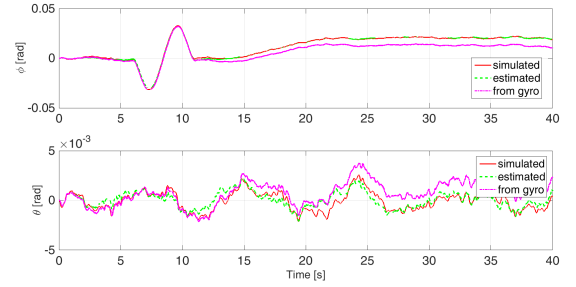


Fig. 6. Attitude tilt angles.

against the GPS noise, spilling into the loop through the position model error. In order to provide the reference

Table 1. Control units parameters.

| Control section        | Order | Complementary eigenvalues $\gamma_k$ |
|------------------------|-------|--------------------------------------|
| <b>State observer:</b> |       |                                      |
| 3D Jerk                | 2     | 0.3 ( $f_s = 2.40 \text{ Hz}$ )      |
| 3D Acceleration        | 2     | 0.2 ( $f_a = 1.60 \text{ Hz}$ )      |
| 3D Position            | 4     | 0.01 ( $f_r = 0.08 \text{ Hz}$ )     |
| Attitude               | 2     | 0.01 ( $f_q = 0.08 \text{ Hz}$ )     |
| <b>Control law:</b>    |       |                                      |
| 3D control law         | 4     | 0.2 ( $f_{min} = 0.80 \text{ Hz}$ )  |

states as well as the reference command, a polynomial reference generator has been used. For the sake of brevity, the reference generator design and tuning is not addressed here. Concerning the target to be achieved, the altitude trajectory is kept constant at 5 m whereas the horizontal desired displacement is of 1 m along the inertia Y-axis (in green in Fig. 5). Figure 5 reports the Y-axis component of the quadrotor inertial position. The position estimate (in red) coming from the 3D observer follows the measurement signal provided by the GPS (in cyan). This implies that the 3D observer works properly. Also, the control law allows the quadrotor to track satisfyingly the reference trajectory (in green). Figure 6 shows the attitude tilt angles ( $\phi$  and  $\theta$ ). The attitude angles obtained through a simple integration of the gyroscope measurements (in magenta) are affected by a drift. By contrast, the tilt angles  $\hat{\theta}$  estimated by the attitude observer (in green) match with the simulated angles (in red). Hence, the attitude observer is able to correctly estimate and reject the gyroscope low-frequency errors through the attitude measurement ( $\hat{\theta}$ ) obtained by the calibrated accelerometer. Figure 7 depicts the time profile of the accelerometer measure ( $\mathbf{y}_a$ ), throughout the mission. It is possible to distinguish the two flight control modes: (i) calibration and (ii) mission. After about 1 s the

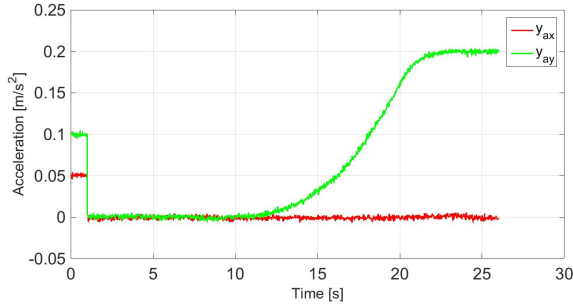


Fig. 7. Accelerometer measurement.

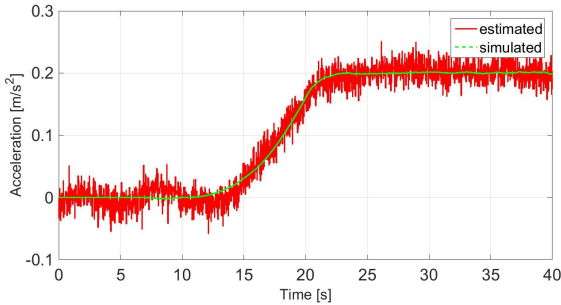


Fig. 8. Position state observer: disturbance estimate.

accelerometer bias is automatically detected and cancelled. Therefore, switching to the mission mode, the accelerometer loop and the attitude loop are finally closed with the calibrated accelerometer measurement. On a final note, a reliable estimate of the external acceleration disturbances affecting the quadrotor in flight (e.g. the simulated nearly-constant horizontal wind in Fig. 8) are retrieved from the 3D observer estimated states.

## 5. CONCLUSION

In summary, in this study the extent to which the Embedded Model Control methodology may be applied to the control of a quadrotor UAV was studied. The Embedded Model Control is a model-based control technique, based on a simplified model of the plant, allowing the estimation and rejection of a wide range of disturbances affecting the quadrotor in flight. Hence, the feedback linearization technique was applied to the non-linear quadrotor model due to its capability of providing a simple linearized model by collecting all the non-linearities at the command level. This structure fits perfectly with EMC because such non-linearities can be estimated as disturbances and then rejected.

The feedback linearized model needs an estimate of the quadrotor attitude. Therefore, the quadrotor attitude has been reconstructed through a proper state observer, which provides a tilt estimate which is free from the gyroscope low-frequency errors. Further, an accelerometer bias calibration procedure was performed and successfully tested. The designed EMC control unit was tested with a high-fidelity simulator. The finding indicates that the EMC control unit, based on the feedback linearized model, works properly and allows the quadrotor to follow the desired flight trajectory.

Future work should evaluate, by simulation, the impact of the propeller model on the control unit performance level.

## REFERENCES

- Alexis, K., Papachristos, C., Nikolakopoulos, G., and Tzes, A. (2011). Model predictive quadrotor indoor position control. In *2011 19th Mediterranean Conference on Control and Automation, MED 2011*, 1247–1252. doi: 10.1109/MED.2011.5983144.
- Benallegue, a., Mokhtari, A., and Fridman, L. (2006). Feedback linearization and high order sliding mode observer for a quadrotor UAV. In *International Workshop on Variable Structure Systems, (VSS'06)*, 365–372. doi: 10.1109/VSS.2006.1644545.
- Canuto, E., Montenegro, C.P., Colangelo, L., and Lotufo, M. (2014a). Active Disturbance Rejection Control and Embedded Model Control: A case study comparison. In *Proceedings of the 33rd Chinese Control Conference*, 3697–3702. IEEE. doi:10.1109/ChiCC.2014.6895554.
- Canuto, E., Montenegro, C.P., Colangelo, L., and Lotufo, M. (2014b). Embedded Model Control: Design separation under uncertainty. In *Proceedings of the 33rd Chinese Control Conference*, 3637–3643. IEEE. doi: 10.1109/ChiCC.2014.6895544.
- Hoffmann, F., Goddemeier, N., and Bertram, T. (2010). Attitude estimation and control of a quadcopter. *Intelligent Robots and Systems (IROS), 2010 IEEE/RSJ International Conference on*, 1072–1077. doi:10.1109/IROS.2010.5649111.
- Lee, D., Kim, H.J., and Sastry, S. (2009). Feedback linearization vs. adaptive sliding mode control for a quadrotor helicopter. *International Journal of Control, Automation and Systems*, 7(3), 419–428. doi: 10.1007/s12555-009-0311-8.
- Leishman, R.C., Macdonald, J.C., Beard, R.W., and McLain, T.W. (2014). Quadrotors and Accelerometers: State Estimation with an Improved Dynamic Model. *IEEE Control Systems*, 34(1), 28–41. doi: 10.1109/MCS.2013.2287362.
- Madani, T. and Benallegue, A. (2006). Backstepping Control for a Quadrotor Helicopter. *2006 IEEE/RSJ International Conference on Intelligent Robots and Systems*, (January 2016), 3255–3260. doi: 10.1109/IROS.2006.282433.
- Mistier, V., Benallegue, A., and M'Sirdi, N.K. (2001). Exact linearization and noninteracting control of a 4 rotors helicopter via dynamic feedback. In *Proceedings - IEEE International Workshop on Robot and Human Interactive Communication*, 586–593. doi: 10.1109/ROMAN.2001.981968.
- Sebesta, K.D. and Boizot, N. (2014). A real-time adaptive high-gain EKF, applied to a quadcopter inertial navigation system. *IEEE Transactions on Industrial Electronics*, 61(1), 495–503. doi:10.1109/TIE.2013.2253063.
- Voos, H. (2009). Nonlinear control of a quadrotor micro-UAV using feedback-linearization, no. April. Ieee, 2009, pp. 16.V using feedback-linearization. doi: 10.1109/ICMECH.2009.4957154.